01 Jan 1968

Current Density-Anodic Potential Curves Of Single Crystal GaAs At Low Currents In KOH

Martin E. Straumanis
Missouri University of Science and Technology

J. P. Krumme

William Joseph James
Missouri University of Science and Technology, wjames@mst.edu

Recommended Citation

M. E. Straumanis et al., "Current Density-Anodic Potential Curves Of Single Crystal GaAs At Low Currents In KOH," *Journal of the Electrochemical Society*, vol. 115, no. 10, pp. 1050 - 1053, The Electrochemical Society, Jan 1968.
The definitive version is available at https://doi.org/10.1149/1.2410872

Current Density-Anodic Potential Curves of Single Crystal GaAs at Low Currents in KOH

Current Density-Anodic Potential Curves of Single Crystal GaAs at Low Currents in KOH

M. E. Straumanis,* J. P. Krumme, and W. J. James*

Graduate Center for Materials Research,
Departments of Metallurgical Engineering and Chemistry, at The University of Missouri-Rolla, Missouri

ABSTRACT

Single p-type, GaAs crystals of high purity, Zn doped, were used to determine whether or not the inverse octahedral {111} faces show potential differences and various rates of anodic dissolution. The Ga{111}, As{111}, {110}, and {100} faces, were polished, etched, and etch-polished with concentrated H_2SO_4 + H_2O_2, and immersed in 1*N* KOH. The Ga{111} faces were found to be the most noble with respect to rest and anodic dissolution potentials. The potential difference between the inverse {111} faces was as large as 0.14v for the rest and 0.123v for the dissolution potentials. The 4 anodic polarization curves gave nearly parallel Tafel lines, with a slope of 66.0 ± 1 mv/log *i*, up to current densities of 0.5 ma/cm^2. The rate of anodic dissolution of the As{111} faces was 69 X as high as the inverse Ga{111}. The activation energies of dissolution of all 4 faces were equal within experimental limits: 16.7 ± 0.7 kcal mole^{-1}. It is concluded that the slow step in the dissolution of GaAs is a one electron discharge with subsequent steps leading to the formation of $Ga(OH)_3$ to provide a protective coating not readily soluble in KOH. From this point of view all observed phenomena can be explained in a qualitative manner.

Crystals without a symmetry center are polar; the polarity shows up through differences in chemical and physical behavior of the inverse planes of the respective crystals. The cubic III-V semiconductor compounds of diamond-type structure belong to this class, of which the best known are GaAs and InSb. Their polarity is displayed by the behavior of the inverse octahedral planes III{111} and V{111}, *e.g.*, GaAs by Ga{111} and As{111}.

Reaction of III-V semiconductors in various media, with or without applied current have been studied by Gatos *et al.* (1), Pleskov (2), Gerischer (3, 4), Harvey (5), Brummer (6), Arthur (7), and others (8). They found that the various crystal planes react differently in aqueous media, such that the III{111} and V{111} inverse planes can be distinguished by the formation of specific etch patterns (1, 3, 8). The distinction can also be made from etching rates (1) from the inclination of etch tunnels produced by an anodic current on the GaAs octahedral planes (the tunnels run perpendicularly to As{111} and at an angle of 20° to Ga{111}) (8), and from LEED patterns (9). Furthermore, the two inverse planes exhibit different activation energies of oxygen desorption (as Ga_2O): 54±4 from the Ga{111} and 42±4 kcal/mole from the As<111> face. Since there is little transfer of charges over the valence bridges (9, 10-13), the Ga atoms on the III{111} side retain their 3-valence electrons, while the As atoms on the inverse side retain 5. All this suggests that the two planes should also develop potential differences in electrolytes.

However, in this respect there are major disagreements. Gatos *et al.* reported that group III{111} planes exhibit more noble electrode potentials than group V{111} surfaces: for instance InSb inverse octahedral planes show a potential difference of 75 and more mv (1). Harvey (5) does not insist on a difference, but examination of his data (Fig. 2-3) reveals that the anodic potentials on Ga{111} are more noble than on As{111} at least up to current densities of 50 ma·cm^{-2}. Conversely, Gerischer finds no difference either in dissolution rates or in the current density-potential curves.

Evidently the measurements have not been made under strictly identical conditions. The intention of the present investigation was, therefore, to use high-purity GaAs crystals and to try to get an answer regarding the potentials exhibited in 1*N* KOH by the inverse 111-faces of GaAs, and also by the 110 and 100 planes.

Materials and Preparation of the Electrodes

The single GaAs crystals were obtained from the Monsanto Company (St. Louis, Missouri), grown by the gradient-freeze technique. They were of the p-type containing Zn (<0.5 ppm) as a dopant. The impurity level was less than 1 ppm. The carrier concentration was ~1.6 x 10^{16} cm^{-3}, mobility ~250 cm^2 · volt^{-1} · sec^{-1}, resistivity ~2 ohm · cm, and etch pit density ~800 cm^{-2}. The disks (14-18 mm in diameter, 2-3 mm thick), were cut from the single crystal rod with a wire-blade slicer using a SiC slurry.

The orientation was determined from Laue back reflection patterns and the respective surface planes were adjusted within ±0.5° of the desired orientation by successive grinding of the disks at a certain angle on fine SiC paper wetted with water and rechecking of the new direction with the Laue technique.

The damaged surface layer was removed from each crystal wafer by chemical etching for about 5 min with an aqueous mixture of 1HF (conc.) : $1H_2O_2$ (30%) : $2H_2O$ (by volume). After this operation the polarity of the {111} planes could be determined by comparing the etch patterns with those published in the literature (1, 3, 8).

Scratches, if present, were removed mechanically by polishing on cotton cloth with SiC slurry (600 mesh). Then a chemical polisher $3H_2SO_4$(conc.) : $1H_2O_2$ (30%) was used, which removed all remaining surface irregularities. The polisher has a high viscosity, provides a slow etch rate, and is not as sensitive to concentration changes as is CP4 etchant (mixture of HF, HNO_3, and CH_3COOH). After this treatment the wafers were immediately transferred into dilute HF to prevent precipitation of a surface film, traces of which could be completely removed by dipping the samples into an aqueous solution of EDTA. Finally the wafers were rinsed in water and dried with alcohol. The whole procedure was repeated before any new series of potential measurements. The wafers then had a mirrorlike appearance (Fig. 1). To insure good electrical contact, one side of the wafer (less suited for potential measurements) was vacuum sputtered with Ag at room temperature, so that the impurity

* Electrochemical Society Active Member.

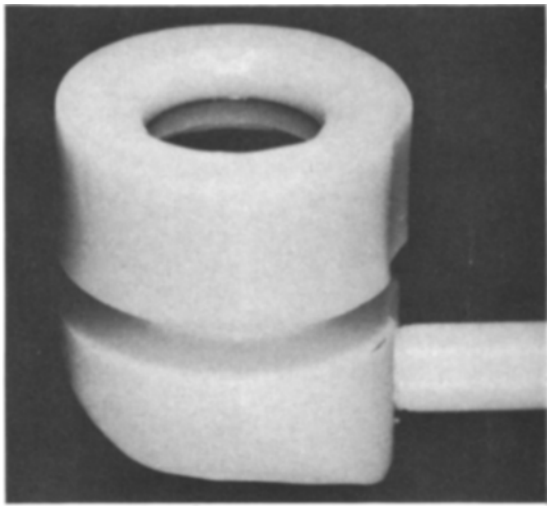

Fig. 1. GaAs wafer in a Teflon holder (electrode)

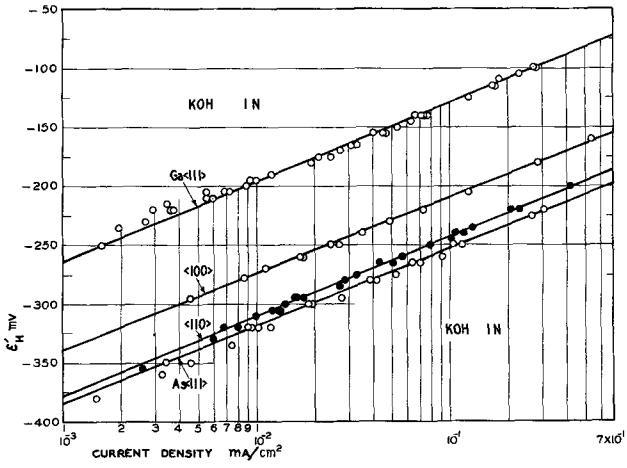

Fig. 3. Anodic dissolution potentials E'_H of GaAs vs. log of current density i of the planes Ga{111}, As{111}, {110}, and {100}. Hydrogen scale; 4°C.

level of the wafer could not be affected by the very slowly diffusing Ag. The contact with the circuit was achieved by Pt foil pressed to the wafer in a Teflon electrode holder (Fig. 1). A section through the holder is shown in Fig. 2. Teflon does not dissolve in the electrolyte (1N KOH) and repels water. The pressure of the screw cap against the wafer was equalized by the use of an O-ring below the Pt foil. Several runs were made on the same sample at current densities below 0.5 ma·cm^{-2} where no surface disintegration of the electrode occurred (8). The potential determining anodic reactions are represented by Eq. [1] and [2]. As the exchange current could only be very small, it was not considered.

Then the electrode was placed in the cell and the potential measurements were made of the GaAs electrode against a 1N calomel reference in a N_2 atmosphere at constant temperatures. Temperatures of 4° and 21°C were selected for the measurements of activation energies. The exposed GaAs surface was between 1.2 and 1.4 cm^2. The electrolyte was vigorously agitated employing a special stirrer and by bubbling N_2 through the electrolyte. The influence of stirring rate on the potentials was not determined.

The d-c power was supplied and the potential controlled by an Anatrol potentiostat. Both power and potential were recorded on a 2-channel recorder on calibrated strip charts.

The chemicals used were all of reagent grade, and the nitrogen was prepurified. The electrolyte (1N aqueous KOH, 1600 ml) was pre-electrolyzed prior to each run using two Pt electrodes at 180 ma (~60 ma/cm^2) over a period of 8 hr. Only traces of Pt could pass into solution and these would not affect the anodic dissolution of GaAs.

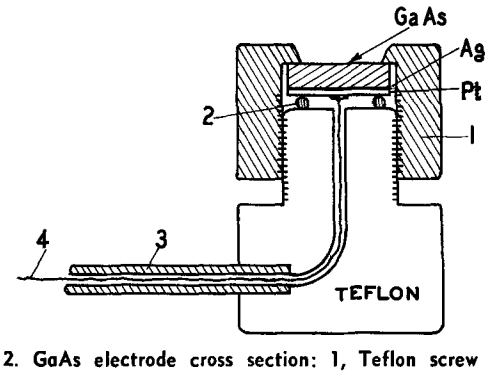

Fig. 2. GaAs electrode cross section: 1, Teflon screw cap; 2, O-ring; 3, Teflon tube (screwed in); 4, lead wire.

Results

Plots of anodic potential *vs.* the log of current density were linear for all the planes investigated (Ga{111}, As{111}, {110} and {100}). All had nearly the same slope, as shown by Fig. 3. The potential measurements for the various planes were highly reproducible. Rest potentials were not as reproducible: —402±40 mv was obtained for As{111} and —262±40 mv for Ga{111}. The $\Delta E'/\Delta \log i$ values for the four planes in the sequence listed above are: 66.7, 65.6, 67.4, and 64.8 mv/log i. They, therefore agree with the values of previous measurements, which usually were between 70 to 95 mv at room temperature (3). In acidic solutions (1N H_2SO_4) they are lower, *e.g.*, 62 mv (5).

The fact that the slope mv/log i on all 4 faces is the same within the limits of error, indicates that the rate-determining step is the same for all the planes subjected to anodic dissolution. The average value of 66.1 mv also suggests that a one-electron charge transfer is involved in the rate-determining step, similarly as for Ge (14, 15).

The activation energies (apparent) were calculated from the Arrhenius equation from the rates of dissolution (current density) at two temperatures (4° and ~21°C), with all other factors remaining unchanged. The values are given in Table I.

Although the measurements were made with two or three GaAs crystals and the planes were etch-polished before each run, the activation energies differ only within the limits of error and, thus, are equal for all crystallographic planes. This result again suggests that the mechanism of dissolution (rds) must be the same on all the crystal faces.

However, Fig. 3 shows that appreciable differences in dissolution potentials do exist. While those exhibited by the As{111} and {110} planes may agree within the limits of error, the largest differences are found between Ga{111} and As{111}, ranging up to

Table I. Activation energies (apparent) of dissolution of various planes of GaAs in 1N KOH at temperatures of 4.0° and ~21°C in kcal mole^{-1}

Plane	Activation energies, kcal mole^{-1}	Average	Max. ± error
Ga {111}	15.8, 16.8, (19.6*), 17.3	16.6	0.8
As {111}	16.6, 16.9, 17.3	16.9	0.4
{110}	17.0, 16.05, 15.8, 16.3, 17.05	16.4	0.6
{100}	15.6, 16.8, 17.3	16.7	0.8
		Average 16.7	±0.7

* Excluded.

0.123v, which is in good agreement with 0.14v, the difference between the rest potentials. The III{111} plane exhibits thereby a more noble dissolution potential than the V{111} plane in agreement with the statements of Gatos *et al.* (1). The potentials of the {100} plane lie in between those of the {111} planes.

It is also apparent from Fig. 3, that the reaction rates on As{111} are highest. For instance, at an anodic potential of —250 mv (hydrogen scale) the rate of reaction on As{111} is about 69 times faster than on Ga{111}, since the current densities developed (16) are 1.1 x 10^{-1} and 1.6 x 10^{-3} ma, respectively.

Discussion

The first important question to be answered is: why are there differences in the rest and dissolution potentials on various faces of the single GaAs crystal, especially between the inverse {111} planes? GaAs, contrary to Ge (14, 15), has a noncentrosymmetric lattice. On etching such a crystal more Ga atoms will be present on one {111} plane whereas on the inverse side more As atoms will be present. This behavior is a consequence of the differential number of valence electrons (3 and 5) of the Ga and As atoms involved. While the bulk of the GaAs structure is, of course, neutral with no charge transfer across the four tetrahedral valence bridges (9-13), a difference in polarity should manifest itself on the outer planes, especially on the inverse {111}, where predominantly either Ga or As atoms are present. This situation causes a considerable difference in the chemical behavior and in the strength of bonding of the surface atoms. In fact, Arthur (7), has shown from O-desorption measurements that the gas is covering both inverse {111} planes; however, the binding state on the Ga{111} is stronger than on the inverse As side. Thus, Ga atoms are the active adsorption centers for O and the latter can be removed from the planes only as Ga_2O (7). There was also evidence for an additional, weaker binding state on As{111} (7). Consequently, the sticking probability of O on clean As{111} faces is greater although the bonding is weaker than on Ga{111} faces, which agrees qualitatively with the LEED measurements (9).

However, oxygen may affect the potential of an anode in two or three ways. Taking, as an example, a metal in which O can be dissolved (formation of a solid solution) the free energy of the metal becomes less negative and its potential more noble (17). The same is also achieved by the development of oxides on the surface, presumably because of a mixed potential (18) formation and/or because of a reduction of the effective surface area. The more adherent and less permeable the oxide layer, the more noble is the potential of the metal. Passivation may eventually occur. Removal of the oxide layer must then result in activation of the metal. This behavior was confirmed by Beck and Gerischer, measuring rest potentials of semiconducting Ge in 0.1*N* NaOH in the presence of air or N_2: in air the potential was considerably more noble (by 393 and more mv) than in N_2 (14). The reversibility of the change from a more noble potential to a less noble and *vice versa* indicated that the oxygen adsorbed on centrosymmetric Ge was rather loosely bound.

It is not known that GaAs dissolves O; therefore, only surface oxides are of importance with respect to surface charges. Since GaAs is noncentrosymmetric, the largest difference in surface arrangement of the Ga and As atoms occurs on the inverse {111} faces. Hence, the adsorption ability of O or of other species of ions such as OH^- (in the electrolyte) by the two faces is not equal. Furthermore, the strength of bonding is influenced by the atomic species. According to Arthur (7) the bonding of O is stronger on Ga{111}, and it should exhibit a more noble potential than the inverse face in aqueous electrolytes. Such a behavior was actually observed not only in air but also in a N_2-atmosphere. In our study a difference of 0.14v for the rest potentials (3.23 kcal) between the two inverse faces was obtained. Therefore, different adsorption products must have been formed on the inverse faces. Figure 4 shows a 110-plane, perpendicular to both 111-planes of the GaAs lattice. On anodic dissolution both atomic species go into solution as trivalent ions (3, 5)

$$Ga \rightarrow Ga^{3+} + 3e \text{ and } As \rightarrow As^{3+} + 3e \qquad [1]$$

the 3*e* being absorbed by the cathode of the d-c source. The reaction of the Ga and As ions with OH^- of the KOH-solution results in colloidal $Ga(OH)_3$ and soluble $As(OH)_3$ or $HAsO_2$ (+ H_2O), which is quickly neutralized by the basic solution to form $KAsO_2$. However, since the dissolution of $Ga(OH)_3$

$$Ga(OH)_3 + KOH \rightarrow KGaO_2 + 2H_2O \qquad [2]$$

is slower and the rate decreases with aging of the colloidal hydroxide, the white hydroxide will be adsorbed by the Ga{111} face. The OH^- might also react directly with the Ga surface atoms, since the Ga bonds are saturated by the bulk of the crystal and the positive charge of the Ga^{3+} is on the {111} surface. $Ga(OH)_3$ adsorption is suggested by the fine, very thin white films observed on GaAs crystals especially on the {110} faces after 3 to 4 hr of anodic dissolution at higher current densities ($\sim$ 1 ma·cm^{-2}). The adherence of the oxide is surely not equal on all the GaAs planes. It is expected that it will be strongest on Ga{111}, although the layer may be thinner than on the {110} face. Thus, even in a neutral gas atmosphere there is a protective layer on Ga{111} (less developed on As{111}) causing a potential difference between the two, the former being more positive. It is impossible at this time to give other than a qualitative characterization of the surface layers. Nevertheless, the layers explain the decreased rate of anodic dissolution of Ga{111} (Fig. 3).

The inverse side is attacked faster because of easy dissolution of $As(OH)_3$ in KOH. However, the closely adjacent layer of Ga-atoms (Fig. 4) dissolves also, as the $Ga(OH)_3$ formed, evidently cannot adhere to the next As row of atoms and, hence slowly dissolves in KOH according to Eq. [2] (formation of gallates). The next As-Ga layer is then attacked in the same way, starting from the dissolving Ga atoms and continuing at higher current densities into the depth of the crystal frequently along etch tunnels perpendicular to the As{111} plane (8). Thus the Ga and As atoms have to go into solution in pairs in accord with the premise of Gerischer (3).

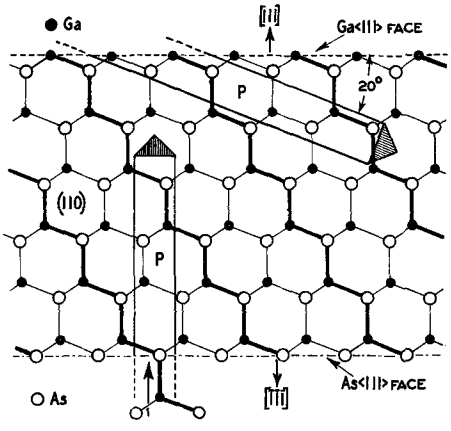

Fig. 4. GaAs{110}-face being in the plane of the page. Both {111}-faces are normal to it. P, primary etch tunnels. The chemical bonds, symbolized by heavy lines, lie in the {110} plane. The arrows represent the direction of the etch tunnels lying in the same plane as the heavy lines (8).

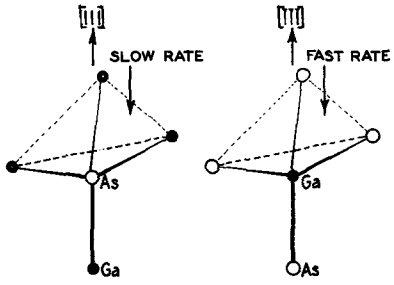

Fig. 5. Various rates of dissolution of Ga atoms on inverse {111} faces.

The Ga{111}-face is partially protected by the slowly dissolving $Ga(OH)_3$ film. Where the latter disappears (reaction [2]) the adjacent As atom also dissolves readily. However, this atom is in the {110} plane at an angle of 20° to the Ga{111}. Therefore, at higher current densities this direction may be that of the etch tunnels (Fig. 4) continuing from Ga to As into the depth of the crystal, which actually was observed (8). Consequently, different etch patterns should be produced on the inverse {111}-planes, in agreement with the photomicrographs (8). The dissolution rates on other crystallographic planes must lie between those found for Ga{111} and As{111} (Fig. 3).

The slope of all the mv/log i lines is the same (Fig. 3) and there is no difference in the activation energies (Table I). The conclusion is, therefore, that the rate-determining step must be the same on all the crystallographic planes. The Ga atoms are those which, because of the reasons mentioned, will remain on any of the dissolving GaAs planes, although starting from the As{111} they will dissolve faster than from the Ga{111} side. Therefore, the dissolution of the complex $Ga\text{-}Ga(OH)_3$ which represents the $Ga(OH)_3$ adsorbed by Ga atoms, should be involved in the over-all mechanism. Depending on where the Ga atoms are in the planes (on faces, corners, or edges of the steps developed during dissolution) and how they are followed by As atoms (Fig. 5), different rates of dissolution on various planes will be developed, although the rate-determining reaction will be the same. The value of the dissolution potential appears then to be dependent on the extent of surface coverage and solubility of the $Ga(OH)_3$.

Therefore, it is expected, that every III-V semiconductor will behave differently during etching and anodic dissolution, depending on the chemical behavior of the atoms in the respective electrolytes.

Acknowledgment

The authors thank the Office of Naval Research for sponsoring the project on dissolution of semiconductors, and the Monsanto Company, St. Louis, especially Mr. J. B. McNeely of the Central Research Department of the company for donation of the GaAs crystals. Thanks are also due to Dr. J. W. Johnson of the Graduate Center for Materials Research for helpful discussions. This paper is Contribution No. 36 from the Graduate Center for Materials Research.

Manuscript submitted April 19, 1968; revised manuscript received ca. May 21, 1968. This paper was presented at the Montreal Meeting, Oct. 6-11, 1968, as Paper 426.

Any discussion of this paper will appear in a Discussion Section to be published in the June 1969 JOURNAL.

REFERENCES

1. *e.g.*, H. C. Gatos and M. C. Lavine, *This Journal*, **107**, 427, 433 (1960).
2. H. W. Pleskow, *Dokl. Akad. Nauk USSR*, **143**, 1399 (1962).
3. H. Gerischer, *Z. Elektrochem.*, **69**, 578 (1965).
4. H. Gerischer, *Z. physik. Chem. N. F.*, **49**, 112 (1966).
5. W. W. Harvey, *This Journal*, **114**, 472 (1967).
6. K. D. N. Brummer, *ibid.*, **114**, 1274 (1967).
7. J. R. Arthur, *J. Appl. Phys.*, **38**, 4023 (1967).
8. J. P. Krumme and M. E. Straumanis, *Trans. AIME*, **239**, 395 (1967).
9. A. U. MacRae, *Surface Sci.*, **4**, 247 (1966).
10. H. Kimmel, *Z. Naturf.*, **20a**, 359 (1965).
11. C. C. Wang and L. H. Spinar, *J. Phys. Chem. Solids*, **24**, 953 (1963).
12. I. I. DeMarco and R. I. Weiss, *Phys. Letters*, **13**, 209 (1964).
13. O. G. Folberth, in H. Welker, "International Conference on Semiconductor Physics," p. 889, Academic Press, New York (1961).
14. F. Beck and H. Gerischer, *Z. Elektrochem.*, **63**, 500, 503, 943 (1959).
15. P. J. Boddy, *This Journal*, **111**, 1136 (1964).
16. K. J. Vetter, *Z. Elektrochem.*, **59**, 596 (1955).
17. W. J. James, W. G. Custead, and M. E. Straumanis, *Corros. Sci.*, **2**, 237, 246, 252 (1962).
18. K. J. Vetter in H. Fischer, K. Hauffe and W. Wiederholt "Passivierende Filme and Deckschichten," p. 249, Springer, Berlin (1956).

Structural Changes During the Anodizing and Sealing of Anodic Aluminas: Intermediate and Far Infrared Analysis

G. A. Dorsey, Jr.

Department of Metallurgical Research, Kaiser Aluminum & Chemical Corporation, Spokane, Washington

ABSTRACT

The longer wavelength far infrared absorptions of anodic coatings are attributed to Al—O—Al or Al—O→Al linkages. Absorption band shifts are found to coincide with changes in anodizing conditions, and these shifts appear to be caused by changes in alumina cross-linking. The effects of anodizing time and current density are examined, as are the effects of sealing: the latter also influencing alumina cross-linking. Apparently, during the formation of these films, there is a relatively short period during which an appreciable quantity of barrier layer converts into the form of the porous layer. Sealing yields a similar conversion.

The intermediate infrared region of from 4000 to ~400 wavenumbers has been widely used for the examination of aluminas. For example, Frederickerson (1) characterized the stretch and bend modes for a number of mineralogical aluminas while Fichter (2) did some earlier work with anodic aluminas. Our own work (3), again with mineralogical aluminas, was used to derive the following correlation chart for the infrared absorptions of hydrous and anhydrous aluminas.

Key words: anodic aluminas, sealing, IR.